

A Public Blockchain-enabled Wireless LoRa Sensor Node for Easy Continuous Unattended Health Monitoring of Bolted Joints: Implementation and Evaluation

Michail Sidorov, Jing Huey Khor, Phan Viet Nhut, Yukihiro Matsumoto, and Ren Ohmura

Abstract— With the advent of Internet of Things (IoT) a slow shift is happening from manual checks of capital intensive assets such as bridges, wind turbines, etc., where bolted joint is used as a main fastening method, towards unattended Structural Health Monitoring (SHM). Numerous approaches are proposed for monitoring the looseness of bolted joint assemblies, however, the majority of them can only be used for looseness detection purposes and not viable for monitoring since these approaches contain design impracticalities, not scalable or hard to implement outside of the laboratory environment. Furthermore, remote unattended monitoring is still very much in its infancy. Thus, to solve this issue, we propose a TenSense M20, a custom designed smart sensor node for continuous remote SHM of bolted joints. Complete node design is presented. Each aspect of the design is evaluated both by simulation and practical tests. Long Range (LoRa) is used as a means of wireless communication and the network can cover 3.8 km. The results show that TenSense M20 is able to precisely track the pre-tension force of a bolted joint with the approach being robust and scalable. Several transmission scenarios are analyzed and in the worst case scenario the node is estimated to last more than 5 years powered by several LiSOCl₂ primary batteries. Received data is securely stored in a blockchain and is easily accessible for services targeting integration with a Smart City.

Index Terms— LoRa, Bolted Joint, Structural Health Monitoring, Internet of Things, Blockchain

I. INTRODUCTION

STRUCTURAL Health Monitoring (SHM) is a method of tracking the health of a structure over its entire lifespan for the purpose of early fault diagnosis and pre-emptive maintenance.

Maintenance managers of capital-intensive assets require a cost-effective and reliable monitoring solution to ensure safety and reliability of these structures. Capital-intensive assets are classified as structures that require a very high amount of initial

investment to be created. These assets include but not limited to planes, bridges, railways, buildings, electric windmill generators, offshore installations, etc. Thus, there is high interest in maintaining these structures in their fully working and safe to operate conditions throughout their entire service life. Majority of these structures use a bolted joint as a main fastening method, which is the simplest, yet an incredibly effective method for fastening two parts of the assembly together. This method, however, is not without drawbacks. Faults can develop over time and the bolt can lose its pre-tension force. Once lost, the bolted joint is unable to serve its main purpose as a fastener i.e. the structure will experience failure, which in turn will not only result in costly repairs, but can also endanger lives. The major types of bolt failure are bolt overload, insufficient pre-load, fatigue, thread stripping, high bearing stress and corrosion. Sources like vibration and environmental effects further contribute to the bolt failure, where the joint usually loses its pre-tension force over time.

In order to prevent failures, scheduled inspections are required. Every country has their own guidelines, however, typically one general inspection per 2-5 years is done [1]–[3]. There is, however, a chance for the fault to develop unnoticed or before the inspection is scheduled. These inspections are costly, still require manual intervention, and are usually not convenient to be performed on remotely located structures. Thus, a different approach is required that enables remote monitoring, logging and subsequent data usage by different services via Internet of Things (IoT). Smart City services for example can utilize this information for notifying drivers and other citizens to execute caution in areas where the structural fault is identified, e.g. on a bridge. For this purpose the data has to be publicly accessible. Currently a number of issues can be identified with IoT systems. They vary in nature, however, the main ones are mostly related to security and cost. Data

This paragraph of the first footnote will contain the date on which you submitted your paper for review. It will also contain support information, including sponsor and financial support acknowledgment.

modification is one of the critical issues in most wireless IoT systems. Thus, to overcome this a lightweight security protocol for SHM systems was proposed to prevent data being modified during the transmission [4]. However, the received data was still stored in a local centralised database and could be changed by attackers, since the systems has a single point of failure. Similarly, storing data on the cloud has the same drawback with an addition of requiring monthly or yearly subscription plan and a risk of data being removed after the expiry of the plan.

To overcome these issues, this paper proposes TenSense M20 - a newly designed IoT sensor node to monitor the pre-tension load of a bolted joint for the purpose of pre-emptive maintenance. System integration with a public blockchain allows for an immutable data storage and provides transparent access for public and Smart City services. The name TenSense is a portmanteau created by combining Tension and Sense, the words that describe the main function of the proposed node - to sense the pre-tension load. M20 denotes the size of the applicable bolt to be used with the current node, and this will be different for the larger size bolts.

The remainder of this paper is structured as follows:

Section II reviews the state of the art approaches aimed at detecting the looseness of a bolted joint.

Section III introduces TenSense M20, a smart node aimed at monitoring the looseness of a bolted joint remotely.

Section IV evaluates the performance of TenSense M20.

Section V integrates TenSense M20 with a blockchain.

Section VI compares TenSense M20 to other solutions.

Section VII concludes the paper.

II. RELEVANT WORK

Numerous approaches for detecting the looseness of a bolted joint assembly are proposed. For better classification they are divided into two big groups, namely In Situ and Unattended. In situ methods are applicable only for on-site diagnostics, meaning the personnel responsible for the check has to be present in front of the bolted joint assembly. Unattended methods, on the other hand, do not require this kind of intervention.

A. In situ monitoring approaches

Currently in situ approaches dominate. We can distinguish a number of groups, based on the looseness detection methods.

1) Computer Vision-based (CV) techniques

These techniques leverage CV for identifying the looseness of the bolt by comparing a series of images of the tightened and loosened bolt. The final result is presented for the assessment after applying the necessary image processing techniques. Park *et al.* demonstrated this by utilizing a Hough transform for feature extraction to identify the rotational angle of the bolt [5]. A change in the angle signified the change in the pre-tension load. Cha *et al.* has improved the aforementioned method and proposed a linear support vector machine for building a classifier capable of automatically differentiating the tightened and loose bolts [6]. Although a better detection rate was

claimed, the method still had its limitations. Thus, Zhao *et al.* has further improved it [7].

Unfortunately, these methods require an on-site inspection, and a database of the initial state of the bolts head. Furthermore, when the bolt initially starts to lose its pre-tension load the rotational angle between the nut and bolt is very small, which cannot be identified. Internal bolt cracks are impossible to detect and the true pre-load value is also impossible to determine.

2) Acoustic Wave-based techniques

These techniques include an actuator to generate, propagate and receive an acoustic wave. The most widespread approach utilizes Piezoelectric Lead Zirconate Titanate (PZT) transducers and a time reversal wave based technique for quantifying the bolts looseness as demonstrated by Parvasi *et al.* [8]. However, the method was prone to saturation, where additional pre-tension force applied does not increase the voltage peak invalidating the reading. Thus, Yin *et al.* proposed a solution by integrating PZT sensors into concave and convex annular disks eliminating the saturation point [9]. Huo *et al.* proposed another PZT based washer [10] with the placement similar to Parvasi *et al.*

Unfortunately, all of these methods need bulky external circuitry to operate the sensors and to process the received information. Apart from a PC in all of the cases a pre-amplifier and a National Instruments DAQ acquisition card were used, making them impractical for low cost deployment.

3) Ultrasonic-based techniques

These techniques use one ultrasonic transducer acting as an actuator and receiver at the same time. In order to perform the measurement the transducer is attached to the head of the bolt and an ultrasonic pulse is generated. This pulse travels through the bolt and is reflected back once it hits the end of the bolt. The total pulse transit time is then determined and compared to known values to evaluate the health of the bolt. Both Bolt Mike III and Dakota Ultrasonics Max II Bolt Tension Monitor utilise this technique [11], [12].

4) Percussion-based approaches

Percussion-based approach is extremely similar to a concept used in clinical examinations for health diagnosis. By listening to the sound emitted after the impact it is possible to detect abnormalities, as loosened structures will emit a sound of a different frequency. Kong *et al.* proposed to use a smartphone for recording this sound and used some processing algorithms to identify the bolts looseness [13]. Similarly, Chen *et al.* used an accelerometer to capture the response signals and processed them in a similar way [14]. Yuan *et al.* used the same approach for sound recording as Kong *et al.*, however, for the looseness identification an intrinsic multiscale entropy analysis was applied with some machine learning techniques [15].

Unfortunately, while providing an interesting opportunity for detecting the looseness, these approaches will not show the true pre-load of the assembly, and monitoring is fairly implausible to achieve.

5) Fiber Bragg Grating-based (FBG) approaches

These approaches rely on an FBG sensor, which is a resonant microstructure typically several millimetres in length photo inscribed inside of a single mode optical fiber. Once a broadband light passes through the structure a portion of it is reflected back at the Bragg wavelength. This wavelength depends on the period of the structure, thus stretching or compressing the structure will change the wavelength, a property used to detect the pre-tension force. FBG sensors are immune to Electromagnetic Interference (EMI), radio frequency interference, they have miniature dimensions, light weight, safe to be operated in hazardous environments, and have high sensitivity and reliability. Yeager *et al.* successfully demonstrated a monitoring of a fasteners pre-load in a composite material [16]. Huo *et al.* and Chen *et al.* integrated FBG sensors in a washer for monitoring purposes [17], [18]. In all of the cases a linear correlation between the applied force and the change in wavelength was observed.

While FBG sensors provide numerous benefits and are inexpensive, they require costly fiber optic interrogators. Furthermore, not all of the benefits provided by FBG sensors will be beneficial for typical SHM.

6) Invasive methods

These methods require some sort of adjustment either to the target structure or the bolt itself, e.g. strain gauge integration into the bolt is a popular approach [19]. An integration of a PZT material inside the structure of the bolt was also demonstrated [17]. Furthermore, an FBG sensor was also fused with a fastener [18].

7) Other

Boltsafe Continuous Monitoring System (CMS) and Periodical Monitoring System (PMS) force washers [20], [21], and colour changing Smartbolts [22] fasteners are among commercially available solutions on the market. However, these products are not suitable for remote monitoring and would require an on-site inspection.

B. Remote monitoring approaches

These methods try to solve the biggest drawback of in situ approaches which is the requirement of an on-site diagnostics by the maintenance crew. However, extremely limited research and development is done in this area with only a few systems existing, e.g. proposed by Mekid *et al.* and Baroudi *et al.* [23]–[27]. These systems, however, used either invasive methods or had design impracticalities. Another paper described a system embedded in a custom designed washer [4]. However, the major limitation of the design was its incapability of being used for smaller than M30 sized bolts and a poor transmission coverage, lowering the scalability of the approach.

C. Contribution of this work

While majority of the above in situ approaches state that they are suitable for monitoring, they are more suitable only for detection purposes. This is true for all CV-based and percussion-based approaches. Invasive methods are undesirable in general, since they will change the property of the fastener,

making it not to conform to already passed standards, i.e. DIN, ANSI or ISO. FBG sensors require expensive and bulky circuitry to operate. Same is observed for PZT-based approaches. Current remote monitoring approaches still require work. Thus, to combat these drawbacks, we contribute by proposing a new cost-effective and scalable solution to continuously monitor the health of bolted joint assemblies. We validate our design using simulation and practical tests. We further propose an integration of the system with a public blockchain to enable the immutable data storage and provide a transparent access for Smart City services to the SHM data.

III. TENSENSE M20 DESIGN

Our system was build ground up and the design was split into two main design parts, namely mechanical and electronic designs. Proper mechanical design and evaluation ensure the integrity of the TenSense M20 structure, while proper electronics design and evaluation provides a guarantee in precision pre-tension force measurement, tracking, and long range wireless communication means. The following design specification for the TenSense M20 was set:

- 1) Precision tracking of pre-tension load
- 2) Successful logging and transmission of the pre-tension value on a scheduled basis
- 3) Sufficient lifetime of the node of at least 5 years
- 4) Design scalability, e.g. support of different size bolts
- 5) Transmission coverage of at least 2 km
- 6) Secured and easy accessible monitoring data for Smart City services via blockchain integration

A. Mechanical Design

There are two main mechanical design components that make up the TenSense M20. These are the main custom designed TenSense M20 washer, and the cover assembly, Fig. 6. The cover houses the majority of the electronics, while the washer has the sensors installed. In order to evaluate structural integrity of the washer prior to manufacturing we have simulated the stress distribution by using Finite Element Analysis (FEA). LUSAS package was used for this purpose, with the wireframe model created as seen in Fig. 1. Austenitic stainless steel SUS304N2-X with a minimum yield strength of 450 MPa was chosen as the main material due to its corrosion resistance, toughness and fatigue properties. The general stress distribution obtained via simulation will show us if the custom washer is safe under the pre-tension load. This value has to be lower than the yield strength of the chosen stainless material. The following table shows the important parameters used for the simulation model, Table I. The pre-tension force experienced by the bolted joint in real world applications with M20 bolts is in the region of 180 kN. The simulation results in Fig. 2. show that the general stress distribution is below 200 MPa with the main concentration at the base of the washer. This is well below the yield strength of 450 MPa for our chosen material and proves that the TenSense M20 washer is theoretically safe under the pre-tension load and is suitable for

manufacture, Fig. 3. The integrity will be further validated by practical tests in Section IV.

TABLE I
STAINLESS MATERIAL PARAMETERS USED FOR THE SIMULATION

Property	Value
Young Modulus	200 GPa
Poisson's Ratio	0.3
Density	7930 kg/m ³
Yield Stress	450 MPa

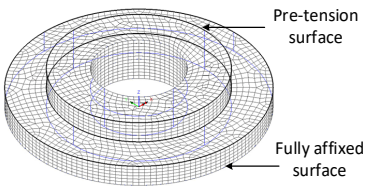


Fig. 1. Wireframe model of the TenSense M20 washer used for FEA.

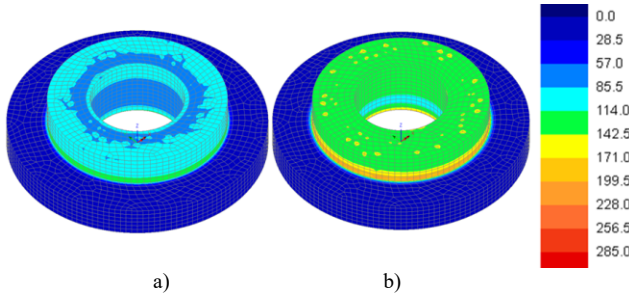


Fig. 2. Stress distribution in a TenSense M20 washer obtained via FEA at (a) P = 91 kN (b) P = 182 kN load, showing that it is lower than the yield strength of 450 MPa for SUS304N2-X stainless material.



Fig. 3. (a) Milled TenSense M20 washer from SUS304N2-X material. (b) Strain gauge placement for the compression experiment.

B. Electronics Design

Main blocks that build up the overall electronics system are the Control Module, the Power Delivery, the Force Measurement circuitry, and some miscellaneous Sensors. The complete system diagram can be seen in Fig. 4.

A Murata CMWX1ZZABZ-078 Long Range (LoRa) and Long Range Wide Area Network (LoRaWAN) capable main module is used in the design as the main component responsible for interfacing the sensors and for wireless communication. It integrates both STM32L082 microcontroller based on an ARM Cortex M0+ architecture and a Semtech SX1276 LoRa transceiver [28]. LoRa, being an Low Power Wide Area Network (LPWAN) protocol, was chosen as means of communication due to numerous reasons, e.g. lower power requirement compared to other LPWAN protocols i.e. Random

Phase Multiple Access (RPMA) [29], Sigfox [30], and cellular protocols i.e. Narrow Band IoT (NB-IoT) [31] and Long Term Evolution for Machines (LTE-M) [32]. The second criteria is transmission coverage. LoRa should be able to provide coverage of up to 15 kilometres, which is sufficient for our application. Cellular protocols provide a better coverage, since the infrastructure is already in place. However, SIM card and a data plan are required inherently increasing the running costs.

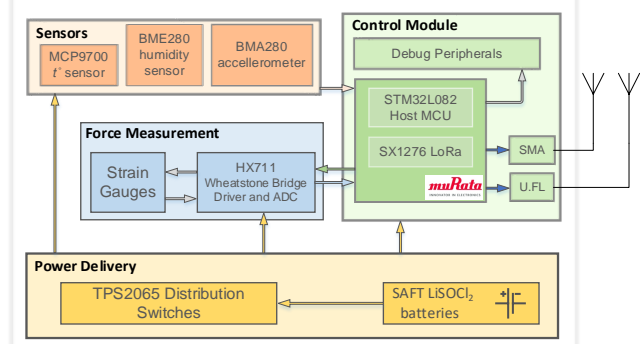


Fig. 4. Block diagram of the TenSense M20 end node electronics.

The whole circuitry is assembled on a single custom designed PCB, with the layout and assembled PCB pictured in Fig. 5a and 5b respectively. Fig. 6 shows both the internal structure of the node and the assembled prototype. Strain gauges are used as a means of sensing the pre-tension force and are accurate if used correctly.

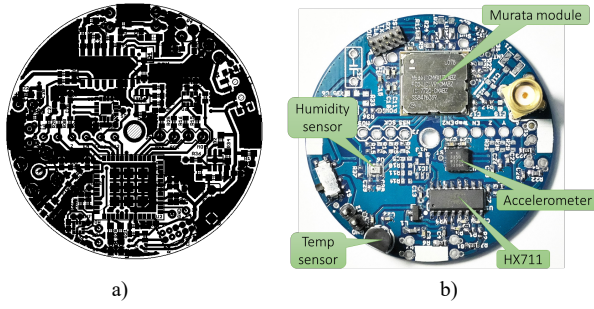


Fig. 5. (a) TenSense M20 PCB layout (b) Assembled TenSense M20 PCB for testing purposes.

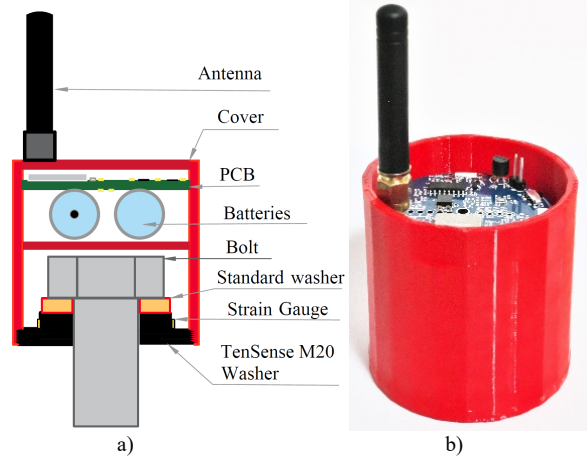


Fig. 6. Node overview (a) Overall design (b) Assembled prototype. Top cover is removed to expose the PCB for illustration.

They change their resistance in proportion to the external force applied. When configured in a Wheatstone bridge, Fig. 7, with a DC voltage applied across, it is possible to sense this change, albeit the change in voltage is measured. R1 - R4 depict the resistors, while G1 - G4 represent the strain gauges, and V_{out} is the output voltage of the Wheatstone bridge. Ideally, in the equilibrium state, when the bridge is balanced, i.e. all resistances are equal, the output voltage V_{out} of the bridge is equal to 0 V. Practically, due to component tolerances, this is never the case. Thus, calibration in software is necessary.

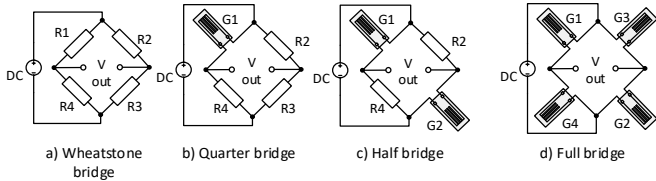


Fig. 7. Wheatstone bridge configurations: (a) Basic Wheatstone bridge (b) Quarter bridge with one active strain gauge (c) Half bridge with two active strain gauges (d) Full bridge with four active strain gauges

A change of resistance in one of the legs will directly affect the output voltage of the bridge. For TenSense M20 FLA-1-11-3LJC strain gauges were used with a resistance of $118.5\ \Omega$ and a gauge factor of 2.14. Placement can be seen in Fig. 3b and 6a. They were configured in a half bridge, a configuration that provides a higher sensitivity for our measurements, compared to the quarter bridge. HX711 IC is used for driving the bridge and reading the gauges. It was chosen as a convenient one chip solution compared to the traditional way which requires a separate regulated excitation source, an operational amplifier and an a high precision Analog to Digital Converter (ADC). A number of TPS2065 switches are used to power gate the sensory peripherals and HX711 when not in use to save energy. Design supports antennas with SMA or U.F.L interfaces. RF path is selectable via $0\ \Omega$ resistors and only one path can be used at a time.

IV. PRACTICAL SYSTEM EVALUATION

The system evaluation consists of a number of practical tests necessary to validate the performance of TenSense M20 node. The following briefly describes these tests:

- *Pre-tension load tracking.* Evaluates both the structural integrity of the TenSense M20 washer and the pre-tension load tracking performance of the system.
- *Tracking linearity compared to the simulation data and a reference logger.* Compares the results to the reference.
- *Dealing with environmental fluctuations.* Discusses the environmental effects on the system and evaluates the countermeasures taken.
- *Wireless transmission coverage.* Evaluates the coverage area based on different LoRa settings.
- *Battery life estimation.* Estimates the battery lifetime based on the available current budget, working environment, and pre-determined operating scenario.

A. Pre-tension Load Tracking

This experiment tests both the physical integrity of the washer and the fasteners pre-tension load tracking performance. The following shows the setup for this experiment, Fig 8. For this experiment MRA-100-F2 Universal Testing Machine was used in a compression mode for applying force to the washer. TenSense M20 node was calibrated prior to the experiment. A pre-determined loading profile was used where the machine cycles between gradual loading and de-loading of the sample. The applied force by the machine is recorded and then compared to the reading made by TenSense M20. The following illustrates the tracking performance, Fig 9.

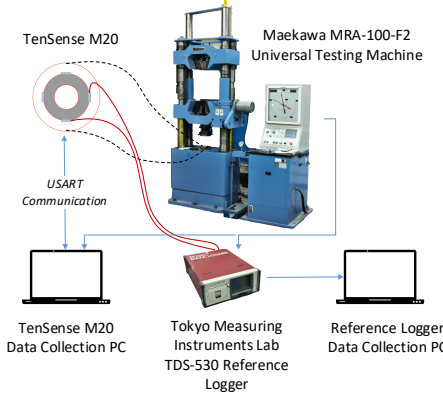


Fig. 8. Test setup used to evaluate the performance of the TenSense M20 node.

Compared to the design presented in [4] the graph shows a more uniform pre-load tracking across the whole range, especially when the low amount of force is applied. In the worst case scenario the tracking delta is less than 2 %. This can also be observed from Fig. 10.

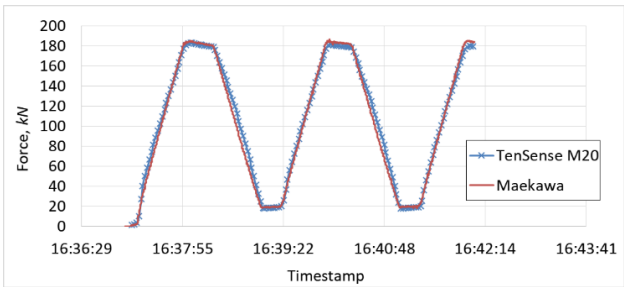


Fig. 9. Tracking performance of the TenSense M20 node based on the pre-defined profile.

B. Tracking Linearity

The strain propagation in a stainless material is directly correlated to the force applied and exhibits a linear behaviour. Thus, we have compared TenSense M20 both to the simulation results obtained via FEA and the measurement done by a reference Tokyo Measuring Instruments TDS-530 logger. For this experiment TenSense M20 reading was changed to display strain value. The strain value from the simulation was extracted at the mounting point of the strain gauges. TenSense M20 shows a lower deviation and a more linear response to the force applied, closely approaching the simulation results, which is a desired outcome, Fig 10.

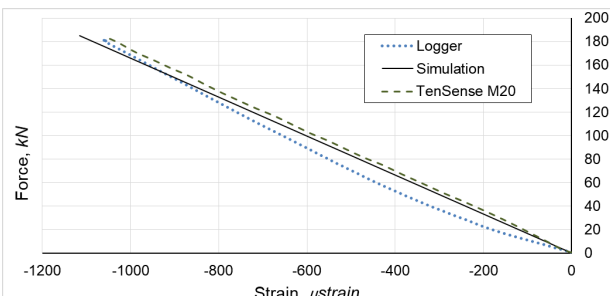


Fig. 10. Linearity of tracking. TenSense M20 compared to the simulation results and the Maekawa reference logger.

C. Dealing with Environmental Fluctuations

Since the node is targeted for outdoor operation environmental factors like temperature swings and weather conditions had to be accounted for. Temperature can affect both the stainless material and electronics i.e. strain gauges and batteries specifically. Every strain gauge type has a different response to strain given a different temperature and this response is not linear. This effect, in our case, can be considered as a sensor drift. Thus, every manufacturer provides a response curve, which can then be used for compensation. TenSense M20 has an inbuilt temperature sensor which is used to apply an offset to the final measurement according to the strain gauge curve. Furthermore, steel can experience elongation. Thus, over a long period of time there can be a slight variation in the measured pre-tension force which is not a concern at this point as the correlation due to thermal expansion is linear.

Majority of the batteries are sensitive to temperature swings. Not only it affects their output voltage, but also the capacity, which degrades in low temperatures, e.g. for primary lithium batteries this degradation can reach 30% of the total capacity. In Japan the node can easily heat up to 60°C during summer and cool down to -30°C during winter. Thus, we have utilised several LS14250 primary lithium-thionyl chloride (LiSOCl₂) batteries manufactured by SAFT due to their wide operating temperatures of -60°C to 85°C, good current handling capabilities, and long shell life according to [33].

To protect the electronics from accidental internal condensation a conformal coating was applied to the PCB during the final stage of assembly.

D. Transmission Coverage

LoRa protocol by design allows either higher speed communication or a larger area coverage. This depends on the duration of the chirp, i.e. Time on Air (TOA), e.g. the time it takes to transmit (TX) the message, which is defined by the Spread Factor (SF), Bandwidth (BW), and the overall size of the message. Our current message consists of a preamble and 11 byte payload containing Node ID, measured Force and Temperature of the washer, Fig. 11.

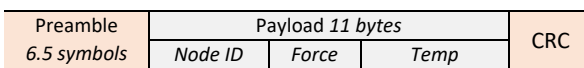


Fig. 11. Complete LoRa frame structure.

By using a half wavelength coiled antenna mounted on TenSense M20, as pictured in Fig 6., and a +20 dBm power mode set both for the node and the receiver station we have measured the TX distance. Experimental results compiled in Table II include TX distance dependency on the SF and BW, and estimated battery lifetime, based on the TX scenario explained in subsection E. Drawback of a better coverage is the longer TOA, which theoretically doubles each time a higher SF is used, directly affecting the battery life, since double the energy is used for TX. Theoretically, the communication distance should double as well, however, this only applies for a direct line of sight, which practically is never achieved.

TABLE II
TRANSMISSION COVERAGE AND EXPECTED BATTERY LIFETIME

SF	TOA, ms	BW, kHz	TX Distance ¹ , m	Current Consumption per TX, mA	Estimated Battery Lifetime ² , years
SF7	29.95	125	2000	0.001065	≤ 33
SF8	59.9	125	2340	0.002130	≤ 27
SF9	119.8	125	2540	0.000426	≤ 20
SF10	198.6	125	2850	0.000706	≤ 15
SF11	397.3	125	3300	0.00142	9.13
SF12	794.6	125	3820	0.00284	5.12
SF12	397.3	250	3600	0.00142	9.13

¹ Applicable only for our test scenario at 15°C temperature, 40% relative humidity level and clear weather conditions.

² Calculated for TX period of 12 times per day.

A higher BW reduces the TOA by a factor of 2, at the expense of a slightly lower coverage, since the sensitivity of the receiver is decreased lowering the link budget. However, not all countries allow BW setting higher than 125 kHz for continuous use, thus, cannot be implemented everywhere [34].

E. Battery Lifetime Estimation

Apart from temperature, battery lifetime depends on the battery type, its capacity, transmission scenario, and the pulse current required by the electronics. High pulse current drain degrades the battery lifetime further contributing to a lower overall current budget. Our system demands up to 130 mA of pulse current during the transmission time at +20 dBm power setting. Thus, several LS14250 batteries were connected in parallel inherently increasing the overall current budget and pulse load handling. The nominal capacity of a single battery is 1200 mA, taking into account the self-degradation imposed by temperature at -30°C, our worst case scenario current budget is 30%, i.e. 720 mA. The following describes the working scenario of the node, with the current draw during each sequence. Assuming the node measures and transmits 12 times per day at +20 dBm power mode, going into sleep afterwards, the lifetime of TenSense M20 can be easily calculated. Three working states are defined, namely ON, TX, and Sleep, Fig. 12. In On Mode the node takes the measurements which takes 1 second. In TX mode the node transmits them to the base station taking from 29.95 ms to 794.6 ms, depending on the BW and SF used.

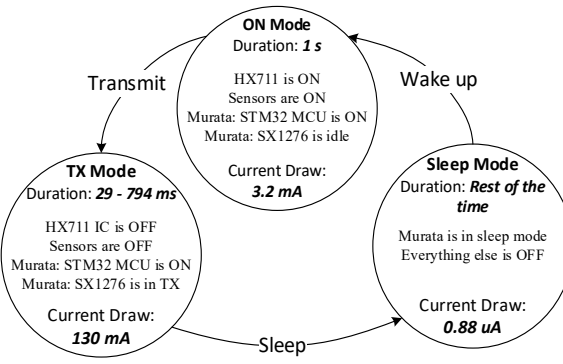


Fig. 12. TenSense M20 operating modes describing the ICs that are turned ON or OFF and respective current draw in that mode.

In Sleep mode HX711 IC and sensors are power gated and the Murata module is in sleep mode until woken up. For our application we have chosen a SF of 12, as this provides larger coverage and a better signal penetration into buildings, and BW of 125 kHz. With the TX period of 12 times per day and the worst case current budget scenario this resulted in an estimate of 5 years of battery lifetime, Table II., which fulfils our set criteria.

V. BLOCKCHAIN INTEGRATION

As previously described, blockchain provides a secure and immutable means for storing IoT sensor data. This is mainly achieved using a consensus mechanism, which dictates the rules on how the data is stored. The data is distributed across thousands of nodes that all contain the same copy of the information eliminating a single point of failure. Modifications to the stored data become extremely hard due to the nature of the consensus mechanism as opposed to a centralised database. Transparency provided by the public blockchain would enable Smart City services to monitor structures health and raise public awareness in case the fault is detected, guaranteeing on-time maintenance and avoiding accidents.

A. Proof of Concept

A blockchain-enabled SHM proof of concept has been developed and deployed on an Ethereum test network. The complete system architecture can be seen on Fig. 13.

The backend of the blockchain system consists of a smart contract, which is a publicly accessible and immutable program. This program is written in Solidity, and is used to manage data records. Infura was used to establish a connection with a Goerli testnet provided by Ethereum network. Truffle was used to compile the smart contract and deploy it as a bytecode on the testnet. To view the data from the blockchain, a decentralized web application was created using HTML and JavaScript, Fig. 14.

The designed smart contract has a custom type, grouping several variables together, and functions that enable storing and reading the data from the blockchain:

1. Custom defined *Struct sensor* structure stores the received data from the node, i.e. the node ID, temperature, force, and added data such as timestamp, and a transaction hash.

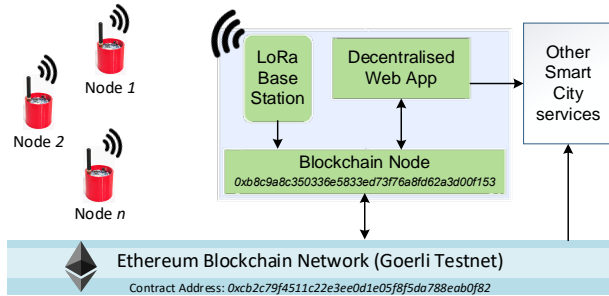


Fig. 13. A complete architecture of the proposed system including the blockchain integration.

TenSense M20 Monitoring Dashboard DEMO				
Available Sensors				
Sensor 1	Sensor 2	Sensor 3		
			Timestamp	Temperature (°C)
Apr-11-2020 20:19:58	20.90	101.00	0x895242beecd109740c6bb8cd21e538bf7f7a5149579958008ed0308796017	
Apr-11-2020 20:14:58	20.80	101.00	0xb78facd3201bd83d9901b71h09d8479f281abe17e674dc3b58979f67365630	
Apr-11-2020 20:09:58	20.60	100.00	0x33909224d4886d161e64cd0c78136dab949e548344705c6f5c49f492248324	
Apr-11-2020 20:05:13	20.50	100.00	0x14df58b25744697ebe05788c0e6225ce831175ad469817734a8e602042f	
Apr-11-2020 19:59:58	20.60	100.00	0xb21b3a4d0hf1a6458617e52beaa58507510c6cf80a3860722c9399583aeb	
Apr-11-2020 19:55:13	20.90	101.00	0x240c62624949070707300efec07ed4b839879f9d86810c12c78319546d0a9	
Apr-11-2020 19:49:58	21.00	101.00	0xb1e677132d952045b6a1f2b79f163ada109e44a7b269c1369j29985ec	
Apr-11-2020 19:44:58	21.20	101.00	0xb5857474d7e8486562e96620e987f1accfc0e592389642573d92edfa244f6	
Apr-11-2020 19:40:13	21.20	101.00	0xf958527a6996e6e172771ab690e801ac94f23603a895c766a1b3132d672	
Apr-11-2020 19:35:13	21.10	101.00	0xe7a47502a7d9196e507301e0fa05c267c91aba58710dd0a00149f696669b	
Apr-11-2020 19:30:13	21.00	101.00	0x3443439fcb7ce2e041d92ca940a4d6549766a5ca1dabd37d10f5e0d896e7	
Apr-11-2020 19:24:58	20.90	101.00	0xd5bb4c45da10fc0f8a73075b89492f7ad54ab108d836ac5472b3c70183fb	

Fig. 14. Interface excerpt of the decentralised web application. Transactions can be found in [35] and [36].

2. A private *setInput* mutator function is used to store the data and prevents it from being accessed by the derived contract. A unique transaction hash is generated upon a successful execution of the *setInput* function and is stored in the *Struct sensor* through an internal *setHash* function.

3. Data is obtained from blockchain using a public *getInput* accessor function, ensuring timestamp, node ID, temperature, force, and transaction hash are transparent to the public.

Each transaction consumes a certain amount of gas, i.e. fuel, which is priced in Gwei and paid in Ether. This payment can be made using MetaMask, serving both as a Hierarchical Deterministic (HD) wallet, and a means of interacting with the web application.

B. Performance Analysis

Performance of the proposed public blockchain-enabled SHM system was analysed based on the data transparency, data modification, and storage cost as follows.

- 1) Data transparency. Data is accessible from Goerli Etherscan via goerli.etherscan.io using either transaction hash [35], the contract address itself [36] or through the decentralized application as shown in Fig. 14. Data on the blockchain is available in a hexadecimal format, Fig. 15.

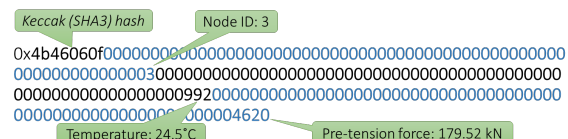


Fig. 15. Available sensor data on the Ethereum Goerli testnet via Etherscan.

2) Data modification. A private *setInput* function prevents attackers to store malicious data in the blockchain. Transaction hash generated for each successful execution of a *setInput* function prevents the content from being modified by attackers. If attackers attempt to modify the transaction content, the generated hash will be different, resulting in the transaction and the node to be rejected from the network. An expected result, since the other nodes have the original unmodified record and will not accept any modifications or deviations due to the consensus mechanism.

3) Storage cost. The gas consumed by executing *setInput* function depends on the data being written to the storage location, however, is in the region of 100000 gas. With the price of 1 Gwei per gas, this gives us the average total transaction cost of 0.00008 ETH. Assuming 10000 transactions are conducted, the transaction cost is 0.8 ETH, which is equivalent to 112 \$ (using the exchange rate of 1 ETH = 140 \$ at the time of writing this paper). However, this cost can be dramatically reduced if the proposed system is migrated to an IOTA blockchain allowing for micro-payments to be executed.

VI. TENSENSE M20 COMPARISON TO RELEVANT WORK

The following table compares the designed TenSense M20 node to the approaches described in the Relevant Work section, Table III.

TABLE III

TENSENSE M20 COMPARISON TO AVAILABLE SOLUTIONS

Criterion	TenSense M20	TenSense M30	FBG	PZT	Percussion	Mekid <i>et al.</i> [27]
Remote Monitoring	Yes	Yes	No	No	No	Yes
Non Invasive Approach	Yes	Yes	Yes	Yes	Yes	No
Continuous Monitoring	Yes	Yes	Yes	Yes	No	Yes
Blockchain Integration	Yes	No	No	No	No	No
Design Scalability	Yes	Ltd. to \geq M30 bolts	Ltd.	No	No	Ltd.
TX Coverage	$\leq 3.8 \text{ km}$	$\leq 0.8 \text{ km}$	NA	NA	NA	Not specified
True pre-load value	Yes	Yes	Yes	Yes	No	Not implemented

Ltd. – Limited

As can be seen TenSense M20 clearly outperforms all of the approaches in the majority of the categories.

VII. CONCLUSION

This paper presented the design and evaluation of a TenSense M20 smart node targeted at remote monitoring of a bolted joint assembly. The proposed approach has achieved all specified goals. Design is scalable and can be easily adapted for usage with larger sized bolts. Miniaturization is also possible

and will allow the use of smaller sized bolts. Evaluation of the node proves that the TenSense M20 washer is safe under pre-tension load. The pre-tension load tracking shows minimum deviation between the applied force by the compression machine and the measured one by TenSense M20 node. The transmission distance is sufficient to cover the monitoring of structures located 3.8 km away from the base station in a suburban environment with an estimated worst case lifetime of the node being more than 5 years. The data transparency provided via blockchain integration can be leveraged by Smart City services to provide a safer living environment via warning notification to its inhabitants when necessary.

The future revision of the node will concentrate on integrating the antenna inside the cover assembly, which will reduce the accidental damage. Other sensors will be utilised for further SHM means that will aid in a broader analysis of the structures health.

ACKNOWLEDGMENT

This project was done in collaboration with our industrial partner Toyo Metal Co., Ltd.

REFERENCES

- [1] Bundesministerium für Verkehr und digitale Infrastruktur, “Bauwerksprüfung nach DIN 1076 Bedeutung, Organisation, Kosten,” 2013.
- [2] New York State Department of Transportation, “Bridge Inspection Manual,” 2016.
- [3] CETV, “Guide d’application de l’instruction technique pour la surveillance et l’entretien des ouvrages d’art,” 2012.
- [4] M. Sidorov, P. V. Nhut, Y. Matsumoto, and R. Ohmura, “LoRa-Based Precision Wireless Structural Health Monitoring System for Bolted Joints in a Smart City Environment,” *IEEE Access*, 2019.
- [5] J. H. Park, T. H. Kim, and J. T. Kim, “Image-based bolt-loosening detection technique of bolt joint in steel bridges,” in *International Conference on Advances in Experimental Structural Engineering*, 2015.
- [6] Y. J. Cha, K. You, and W. Choi, “Vision-based detection of loosened bolts using the Hough transform and support vector machines,” *Autom. Constr.*, 2016.
- [7] X. Zhao, Y. Zhang, and N. Wang, “Bolt loosening angle detection technology using deep learning,” *Struct. Control Heal. Monit.*, 2019.
- [8] S. M. Parvasi, S. C. M. Ho, Q. Kong, R. Mousavi, and G. Song, “Real time bolt preload monitoring using piezoceramic transducers and time reversal technique - A numerical study with experimental verification,” *Smart Mater. Struct.*, 2016.
- [9] H. Yin, T. Wang, D. Yang, S. Liu, J. Shao, and Y. Li, “A smart washer for bolt looseness monitoring based on piezoelectric active sensing method,” *Appl. Sci.*, 2016.
- [10] L. Huo, D. Chen, Q. Kong, H. Li, and G. Song, “Smart washer - A piezoceramic-based transducer to monitor looseness of bolted connection,” *Smart Mater. Struct.*, 2017.
- [11] GE Inspection Technologies, “Krautkramer BoltMike III.” General Electric Company. Datasheet., 2004.
- [12] Dakota Ultrasonics, “MAX II Bolt Tension Monitor.” Dakota Ultrasonics. P/N P-197-0002 Datasheet., 2015.
- [13] Q. Kong, J. Zhu, S. C. M. Ho, and G. Song, “Tapping and listening: A new approach to bolt looseness monitoring,” *Smart Mater. Struct.*, 2018.
- [14] R. Chen, S. Chen, L. Yang, J. Wang, X. Xu, and T. Luo, “Looseness diagnosis method for connecting bolt of fan foundation based on sensitive mixed-domain features of excitation-response and manifold learning,” *Neurocomputing*, 2017.
- [15] R. Yuan, Y. Lv, Q. Kong, and G. Song, “Percussion-based bolt looseness monitoring using intrinsic multiscale entropy analysis and BP neural network,” *Smart Mater. Struct.*, 2019.

- [16] M. Yeager, A. Whitaker, and M. Todd, "A method for monitoring bolt torque in a composite connection using an embedded fiber Bragg grating sensor," *J. Intell. Mater. Syst. Struct.*, 2018.
- [17] L. Huo, D. Chen, H. Li, and G. Song, "The development of a fiber Bragg grating based smart washer," 2018.
- [18] D. Chen, L. Huo, H. Li, and G. Song, "A fiber bragg grating (FBG)-enabled smart washer for bolt pre-load measurement: Design, analysis, calibration, and experimental validation," *Sensors (Switzerland)*, 2018.
- [19] S. Mekid, U. Baroudi, and A. Bouhraoua, "Stand Alone Smart Bolt for e-Maintenance," *Int. J. Eng. Technol.*, 2012.
- [20] BoltSafe, "BoltSafe Sensor CMS." BoltSafe Sensor Continuous Monitoring System datasheet, Version 2.0.
- [21] BoltSafe, "BoltSafe Sensor PMS." BoltSafe Sensor Periodic Monitoring System datasheet, Version 2.0.
- [22] Charles Popeno, "Making The Case For Tension Indicating Fasteners," *Am. Fasten. J.*, 2011.
- [23] S. Mekid and U. Baroudi, "Fastener Tension Monitoring System," US Patent 8,893,557 B2, 2014.
- [24] S. Mekid, B. Abdelhafid, and U. Baroudi, "Smart Lid for Smart Bolts and Probes," US Patent 8,540,468 B2, 2013.
- [25] S. Mekid and B. Abdelhafid, "Bolt Tension Monitoring System," US Patent 8,596,134 B1, 2013.
- [26] U. Baroudi and S. Mekid, "Bolt Tension Monitoring System," US Patent 8,448,520 B1, 2013.
- [27] S. Mekid, A. Bouhraoua, and U. Baroudi, "Battery-less wireless remote bolt tension monitoring system," *Mech. Syst. Signal Process.*, 2019.
- [28] Murata, "LoRa Module Data Sheet." CMWX1ZZABZ-TEMP datasheet, 2016.
- [29] uBlox, "NANO-S100 RPMA module." NANO-S100 datasheet, 2017.
- [30] WISOL, "Sigfox / Sub-1GHz." WSSFM10R1AT datasheet, 2018.
- [31] DIGI, "Digi Xbee® Cellular NB-IoT." NB-IoT Cellular Smart Modem preliminary datasheet, 2017.
- [32] DIGI, "Digi Xbee® Cellular LTE-M." LTE-M Cellular Smart Modem preliminary datasheet, 2017.
- [33] SAFT, "SAFT Primary lithium battery LS 14250." Arthur Associates Limited. Datasheet., 2019.
- [34] LoRa Alliance Technical Committee Regional Parameters Workgroup, "LoRaWAN 1.1 Regional Parameters." 2018.
- [35] Etherscan, "Goerli Testnet Network Transaction," 2020. [Online]. Available: <https://goerli.etherscan.io/tx/0x00db507718510f33f173ba72abc47b70ec80604e7b02d49d3d3f0985c7b0470c>.
- [36] Etherscan, "Goerli Testnet Network Contract Address," 2020. [Online]. Available: <https://goerli.etherscan.io/address/0xcb2c79f4511c22e3ee0d1e05f8f5da788eab0f82>.



MICHAIL SIDOROV is a Ph.D candidate at the Toyohashi University of Technology, Japan working in the field of IoT. He has received his B.Sc degree in Informatics from Coventry University, UK in 2009, B.Sc Degree in Informatics Engineering from Klaipeda University, Lithuania in 2010 and a joined M.Sc degree in Embedded Computing Systems (EMECS)

from Norwegian University of Science and Technology (NTNU), Norway and University of Southampton (UoS), UK in 2013. He was a Teaching Fellow and Laboratory Officer for the period of 2013 – 2017 at the University of Southampton Malaysia. His current research interests include energy harvesting sensor networks, LPWAN, and blockchain technology for IoT.



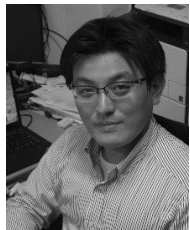
JING HUEY KHOR is an Assistant Professor at the University of Southampton Malaysia Campus. She received her B.Eng degree in Electrical Engineering (Electronic) with First Class Honours from Universiti Malaysia Pahang in 2009. She then received her Ph.D degree for conducting research on Passive Radio Frequency Identification (RFID) security at Universiti Sains Malaysia in 2013. Her research interests include information security in RFID and IoT as well as blockchain technology.



PHAN VIET NHUT is a lecturer at Danang University of Technology, Vietnam and a PhD candidate at Toyohashi University of Technology, Japan. He received his B.Sc degree in Department of Civil Engineering, Danang University of Technology, Vietnam. His research field is the applications of FRPs to civil structures, the development of repair and strengthening for steel structures using CFRP, and the strengthening of FRP connection using thin FRP sheets.



YUKIHIRO MATSUMOTO is an Associate Professor at the Department of Architecture and Civil Engineering, Toyohashi University of Technology Japan. He received his B.E., M.E., and Dr. Eng. degrees from Toyohashi University of Technology, in 2002, 2004, and 2007, respectively. His research field is the fiber-optic sensing for FRP material, the applications of FRPs to civil structures and the development of repair and strengthening for steel structures using CFRP. Dr. Matsumoto is a member of the International Institute for FRP in Construction (IIFC), the International Association for Shell and Spatial Structures (IASS), the Japan Society of Civil Engineers (JSCE), the Architectural Institute of Japan (AIJ) and the Japan Society of Steel Construction (JSSC).



REN OHMURA is an Associate Professor at the Department of Computer Science and Engineering, Toyohashi University of Technology, Japan. He received his Bachelor of Electric Engineering, Master of Computer Science, and Ph.D degrees from Keio University in 1999, 2001, and 2004 respectively. Currently, he runs Ubiquitous Systems laboratory at TUT and supervises students ranging from BSc to PhD level. His research works are on ubiquitous computing, wearable computing, IoT, smart environment, battery-less systems, and distributed systems.